THE IMPACT OF CALIBRATION, SENSOR DIFFERENCES, AND INFORMATION CONTENT ON PRECIPITATION ESTIMATES FROM THE GPM RADIOMETER CONSTELLATION

Wesley Berg, Colorado State University

INTRODUCTION

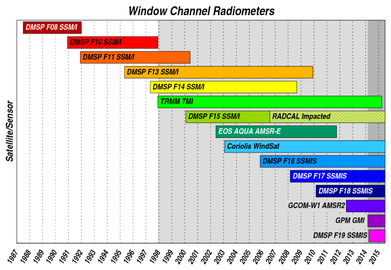

Data availability from the window-channel radiometers. The light gray shaded region corresponds to the TRMM era and the dark grey shaded region to the GPM era.

According to Hou et al. 2014 "The GPM mission is specifically designed to unify and advance precipitation measurements from a constellation of research and operational microwave sensors". This approach takes advantage of existing satellite sensors from many different space agencies, but presents a number of challenges in producing consistent precipitation estimates from radiometers with widely varying capabilities and calibrations. Understanding and addressing the issues leading to differences in precipitation estimates between sensors is critical to accomplish many of the stated GPM science goals. Consistency in the precipitation estimates from the constellation sensors requires physically consistent input brightness temperatures (Tb) between sensors as well as properly accounting for and understanding how differences in sensor characteristics and calibration impact the retrieval apriori database, the retrieval algorithm, and the level 3 merged precipitation products.

Producing consistent precipitation estimates from sensors with different channels and calibrations involves three main components. These include the input brightness temperatures (Tb), the apriori database, and the precipitation retrieval algorithm. For the input Tb, this means ensuring that the calibration of the 22.235 GHz channel on SSMIS is consistent with the 23.8 GHz channel on GMI even though the values will not be the same. Similarly, the apriori database must account for differences in channel frequencies and spatial resolution, and the retrieval algorithm must properly account for time-dependent differences such as the TRMM orbit boost or changes in the Earth incidence angle (EIA). It is important, however, to distinguish the impact of differences in information content between sensors from differences associated with calibration-related errors. The information content is primarily impacted by the channel complement and spatial resolution of the sensor, although noise characteristics, calibration uncertainties etc. can also have an impact. For example, due to its lower orbit and larger main reflector, GMI has much higher spatial resolution than SSMIS, enabling it to distinguish finer features and to better detect small isolated precipitating clouds. GMI also has 10 GHz channels, which don't saturate as quickly as the 19 GHz channels for high liquid water contents enabling GMI to distinguish between profiles in the apriori database containing very intense precipitation. The higher frequency 166 and 183 GHz channels on GMI also provide increased sensitivity to light rain and snow as well as precipitation information over challenging surfaces such as snow on the ground.

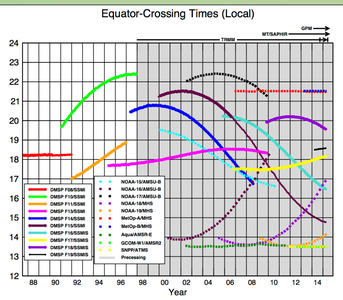

Ascending passes (F08 descending); satellites depicted above graph precess throughout the day. Image by Eric Nelkin (SSAI), 19 May 2015, NASA/Goddard Space Flight Center, Greenbelt, MD.

GPM CONSTELLATION RADIOMETERS

GPM GMI

Satellite/Instrument Characteristics

Nominal EIA	52.8/49.2
Orbit Inclination	65.0 deg
Local Obs. Time	Variable (Precessing)
Altitude	407 km
Reflector Size	1.22 m

GPM GMI Channel Specifications

GMI Specs	10.65v/h	18.7v/h	23.8v	36.64v/h	89.0v/h	165.5v/h	183+3v	183+7v
DT x CT Res in km	32.1x19.4	18.1x10.9	16.0x9.7	15.6x9.4	7.2x4.4	6.3x4.4	5.8x3.8	5.8x3.8
Beamwidth (deg)	1.72	0.98	0.85	0.81	0.38	0.37	0.37	0.37
NEDT (K)	0.96	0.84	1.05	0.65	0.57	1.5	1.5	1.5
Beam Efficiency (%)	91.1	91.2	93.0	97.8	96.8	96.5	95.2	95.2
Uncorr Nonlinearity (K)	0.2 0.2	0.1 0.1	0.1 0.1	0.5 0.5	0.5 0.5	0.5 0.5	0.5	0.5
Band Width (MHz)	100	200	400	1000	6000	4000	3500	4500
Feedhorns	1	1	1	1	1	1	1	1
Integration Time (ms)	3.6	3.6	3.6	3.6	3.6	3.6	3.6	3.6

GCOM-W1 AMSR2

Satellite/Instrument Characteristics

Nominal EIA	55.0
Orbit Inclination	98.2 deg
Local Obs. Time	1:30 am/pm
Altitude	700 km
Reflector Size	2.0 m
ASC	Automatic Gain Control
A/D Conversion	12 bit

Calibration Error Budget

Cold Calibration Target	< 1.2K
Hot Calibration Target	< 0.3K
Detector Non-linearity	< 5K (max at 150K, 7 GHz)
Scan Bias	< 17K (7 and 10 GHz only)
Spillover	< 11K (< 3.3%)
Cross-Polarization	< 1K
Antenna Emissivity	< 0.25%
Antenna Loss	N/A
Random Noise	N/A

GCOM-W1 AMSR2 Channel Specifications

AMSR2 Specs	10.65v/h	18.7v/h	23.8v	36.5v/h	89.0v/h
DT x CT Res in km	42x24	22x14	26x15	12x7	5x3
On orbit V-Pol	40x23	20x14	20x14	-	-
On orbit H-Pol	40x23	25x14	25x14	-	-
Beamwidth (deg)	1.20	0.65	0.75	0.35	0.15
Beam Efficiency (%)	97.6	98.0	97.8	97.8	98.0
NEDT (K)	0.70	0.70	0.60	0.70	1.20
Nonlinearity (K) at 5°C	1.5 2.0	1.8 1.9	1.3 1.6	1.4 1.2	0.3 1.0
Band Width (MHz)	100	200	400	1000	3000
Feedhorns	1		1	1	1
Integration Time (ms)	2.6	2.6	2.6	2.6	1.3

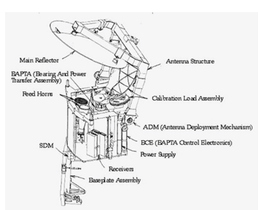

TRMM TMI

Satellite/Instrument Characteristics

Nominal EIA	53.35
Orbit Inclination	35.0
Local Obs. Time	Variable (Precessing)
Altitude	402 km
Reflector Size	61 cm

TRMM TMI Channel Specifications

TMI Specs	10.65v/h	19.35v/h	21.3v	37.0v/h	85.5v/h
DT x CT Res in km	68.1x41.3	34.6x20.9	31.1x18.9	18.3x11.1	7.8x4.8
Beamwidth (deg)	3.68 3.75	1.90 1.88	1.70	1.00 1.00	0.42 0.43
Beam Efficiency (%)	93	96	98	91 92	82 85
NEDT (K)	0.63 0.54	0.50 0.47	0.71	0.36 0.31	0.52 0.93
Band Width (MHz)	100	500	200	2000	3000
Feedhorns	1	1	1	1	1
Integration Time (ms)	6.6	6.6	6.6	6.6	3.3

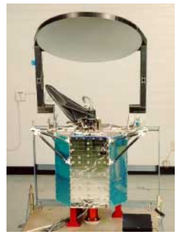

DMSP SSMIS
(F16, F17, F18 and F19)

Nominal EIA	53.1
Orbit Inclination	35.0
Local Obs. Time	F16 -> 20:03 F17 -> 17:32 F18 -> 20:06 F19 -> 18:30
Altitude	833 km
Reflector Size	24" (61 cm)
Nonlinearity	< 0.5 K

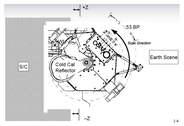

DMSP SSMIS Channel Specifications

SSMIS Specs	19.35v/h	22.235v	37.0v/h	85.5v/h	150h	183+7h	183+3h	183+1h
DT x CT Res in km	74x45	74x45	45x28.5	16x13	16x13	16x13	16x13	16x13
Beamwidth (deg)	1.92 1.94	1.85	1.20 1.19	0.40 0.39				
Beam Efficiency (%)	96.1 96.0	96.2	95.9 96.2	94.4 94.5				
NEDT (K)	0.7	0.7	0.5	0.9	0.88	1.2	1.0	1.25
Band Width (MHz)	400	450	1500	1500	1500	1500	1000	500
Feedhorns	K		Ka	W		G		
Integration Time (ms)	8.4	8.4	8.4	4.2	4.2	4.2	4.2	4.2

*F19 was launched April 2014, but is not yet operational

Microwave Cross-Track Sounders

Satellite Info	NPP ATMS	NOAA 18	NOAA 19	Metop-A	Metop-B	Megha-Tropiques
Launch Date	10/28/2011	5/20/2005	2/6/2009	10/19/2006	9/17/2012	10/12/2011
Inclination	98.7 deg	99.17 deg	98.97 deg	98.7 deg	98.7 deg	19.98 deg
Local Obs. Time	13:30	13:30	13:30	21:30	21:30	Precessing
Altitude	824 km	854 km	870 km	817 km	817 km	870 km
Orbit Period	101.4 min	102.0 min	101.99 min	101 min	101 min	102.15 min

MHS Channel Specifications

MHS Specs	89v	157v	183±7v	183±3h	183±1h
NEDT (K)	0.22	0.34	0.51	0.40	0.46
Band Width (MHz)	2800	2800	2x500	2x1000	2200

SAPHIR Channel Specifications

SAPHIR Specs	183±0.2h	183±1.1h	183±2.8h	183±4.2h	183±6.8h	183±11h
NEDT (K)	2.35	1.45	1.36	1.38	1.03	1.10
Band Width (MHz)	200	350	500	700	1200	200

ATMS Channel Specifications

ATMS Specs	23.8v	31.4v	88.2v	165.5h	183±7h	183±4.5h	183±3h	183±1.8h	183±1h
Beamwidth (deg)	5.2	5.2	2.2	1.1	1.1	1.1	1.1	1.1	1.1
NEDT (K)	0.9	0.9	0.5	0.6	0.8	0.8	0.8	0.8	0.9
Band Width (GHz)	0.27	0.18	2.0	3.0	2.0	2.0	1.0	1.0	0.5

RADIOMETER CALIBRATION

Calibration Corrections

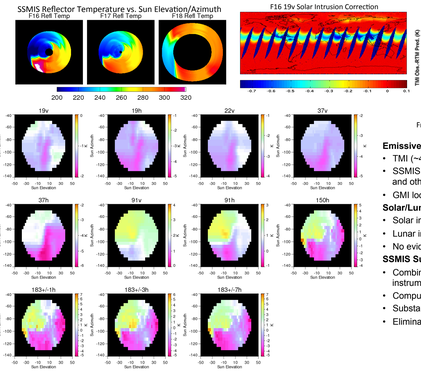

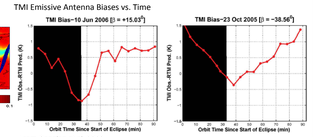

From Gopalan et al. 2009

Emissive Antenna

- TMI (~4% emissivity) correction by UCF applied to 1B11 v7 and GPM L1C
- SSMIS -> Problem for F16 and F17. Difficult to correct for due to intrusions and other issues
- GMI looks good!

Solar/Lunar Intrusions

- Solar intrusions into warm load lead to biases in warm calibration point
- Lunar intrusions into cold-sky mirror bias cold end calibration
- No evidence of significant intrusion issues for GMI

SSMIS Sun-Angle Corrections

- Combined corrections for emissive antenna, solar intrusions, and other instrument temperature-dependent biases
- Computed from multiple years of data using double differences
- Substantial (2-6K) corrections are different for F16, F17, and F18.
- Eliminates biases between ascending and descending orbit passes

Sun-angle dependent corrections for SSMIS on board F17. Note that the patterns are strongly correlated with the reflector temperature (shown above), however, solar intrusions and other thermal effects are also a factor. The magnitude of the corrections for the high-frequency channels are also much larger than for the window channels.

Regional Variability

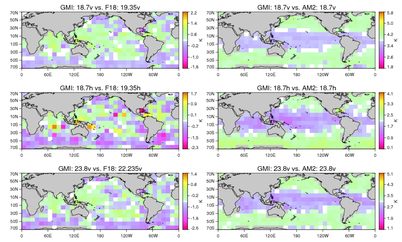

Regional variability of 18v, 18h, and 23v computed calibration offsets (i.e. double differences) for GMI vs F18 SSMIS (left side) and GCOM-W1 AMSR2 (right side).

One of the primary approaches to intercalibrating the constellation radiometers is the double difference technique. This approach uses coincident observations between the reference sensor (GMI) and the target sensor (e.g. AMSR2) matched closely in space and time. The precessing GPM orbit crosses the orbits of the sun-synchronous satellites several times a day. The difference between the observed Tb is then subtracted from the difference between the simulated Tb. The resulting double difference between the observed and simulated (or expected) Tb differences provides an estimate of the calibration difference. Errors in the simulated Tb associated with imperfect estimates of ocean surface and atmospheric state parameters can result in regional patterns in the resulting double differences. We are currently working on developing improved non-precipitating retrievals using the GMI Tb as input in order to reduce these regional errors in the calibration estimates.

Calibration Monitoring

http://rain.atmos.colostate.edu/XCAL

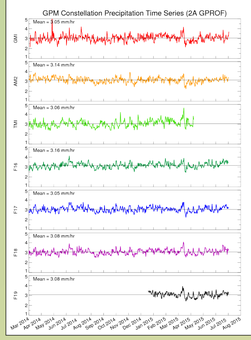

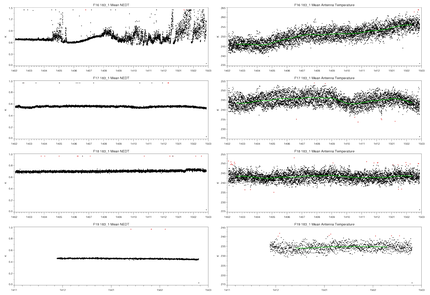

The figure on the left shows time series of mean tropical oceanic precipitation from the operational algorithm for the GPM window channel radiometers. There is some variability associated with extreme events (e.g. hurricanes), but the mean values are very similar and there are no obvious trends.

The above figures show the time series of NEDT (left) and mean antenna temperatures over ocean (right) for the SSMIS 183+/-1 GHz channel on F16, F17, F18, and F19. There is a significant increase in the noise for this channel on board F16 as well as an increasing trend in the antenna temperatures, which is not evident in the same channel from the other SSMIS sensors.

IMPACT ON PRECIPITATION RETRIEVALS

Spatial Resolution and Channel Complement

Window-Channel Radiometers

Table 1: Channel complement in terms of frequency and polarization for TRMM/GPM window-channel radiometers.

Sensor	10 GHz	19 GHz	22 GHz	37 GHz	90 GHz	160 GHz	183 GHz
TMI	10.65 v/h	19.35 v/h	21.3 v	37.0 v/h	85.5 v/h	n/a	n/a
SSM/I	n/a	19.35 v/h	22.235 v	37.0 v/h	85.5 v/h	n/a	n/a
SSMIS	n/a	19.35 v/h	22.235 v	37.0 v/h	91.665 v/h	150 h	183±1,3,6,6 h
AMSR-E	10.65 v/h	18.7 v/h	23.8 v/h	36.5 v/h	89.0 v/h	n/a	n/a
AMSR2	10.65 v/h	18.7 v/h	23.8 v/h	36.5 v/h	89.0 v/h	n/a	n/a
GMI	10.65 v/h	18.7 v/h	23.8 v	36.64 v/h	89.0 v/h	166 v/h	183±3,7 v
WindSat	10.65 v/h	18.7 v/h	23.8 v/h	36.5 v/h	n/a	n/a	n/a

Table 2: Spatial resolution by channel for TRMM/GPM window-channel radiometers.

Sensor	10 GHz	19 GHz	22 GHz	37 GHz	85 GHz	Area Ratio
TMI pre-boost	60x36	30x18	27x17	16x10	7x4	1.0
TMI post-boost	68x41	35x21	31x19	18x11	8x5	1.3
SSM/I	n/a	69x43	60x40	37x25	15x13	5.6
SSMIS	n/a	74x45	73x45	45x29	16x13	6.9
AMSR-E	51x30	27x16	31x18	14x8	6x4	0.9
AMSR2	42x24	22x14	26x15	12x7	5x3	0.7
GMI	32x19	18x11	16x10	16x9	7x4	0.6
WindSat	38x25	27x16	20x12	13x8	n/a	0.5

The most significant differences between the constellation radiometers involve the available channels (i.e. frequencies) and the spatial resolution. A comparison of the channel complements for the TRMM/GPM constellation window-channel radiometers is shown in Table 1 and a comparison of the spatial resolution for these sensors is provided in Table 2. For precipitation retrievals the 10 GHz channels were added to TRMM TMI and subsequent radiometers, while GMI added the high-frequency 166 and 183 GHz channels for sensitivity to rain and snow over land. GMI also has the highest spatial resolution of any of the sensors. The four SSMIS sensors on board F16, F17, F18, and F19 provide substantial temporal sampling over the globe along with the high frequency channels, but have much lower spatial resolution impacting their ability to resolve details within convective storm systems.

Impact of Differences in Sensor Characteristics and Information Content

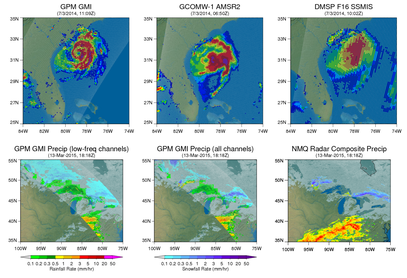

The top row shows a comparison precipitation estimates from Hurricane Arthur from GMI, AMSR2 and SSMIS. The second row shows a comparison of rain/snow estimates from GMI without (low-freq channels) and with (all channels) the high-frequency 166 and 183 GHz channels along with the corresponding NMQ radar composite.

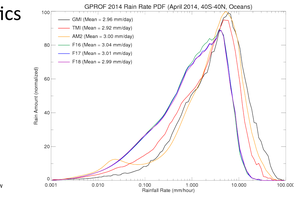

The images of precipitation retrievals from Hurricane Arthur (above left) show the ability of the high-resolution GMI sensor to resolve fine details around the eye, particularly versus the F16 SSMIS sensor. The above figure shows a comparison of the resulting distribution of precipitation intensity from the window-channel radiometers. The lower resolution of the SSMIS sensors dramatically shifts the distribution to the right (lower intensities) as it averages over the larger field-of-view and thus cannot capture the most intense precipitation in the core of convective systems.

The precipitation retrievals shown in the lower row on the left reveal the impact of the addition of the GMI high-frequency channels, particularly for retrieving snowfall. A comparison with gridded NMQ radar estimates in the lower right panel shows significant improvement in the ability of the GMI retrieval to detect both the snowfall area and intensity. These channels are especially important in distinguishing between snow on the ground and falling snow.

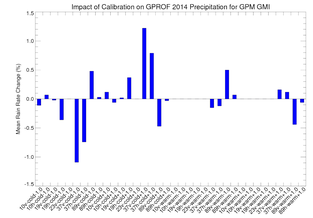

The above bar chart shows the impact of 1K calibration biases for each of the GMI window channels on the precipitation retrieval over oceans. The largest impact is with the 37 GHz channels, particularly the 37v channel at the cold end.

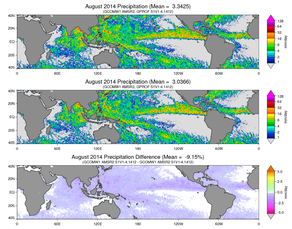

The above figures show the change in precipitation associated with changes in the nonlinearity of the AMSR2 calibration. The top panel corresponds to the original JAXA nonlinearity corrections while the middle panel shows the results using the Remote Sensing Systems (RSS) corrections. The difference is shown in the bottom panel

SUMMARY

1. Intercalibration
   - The latest (i.e. final) GMI calibration looks very good in an absolute sense as well as quite stable, making it an excellent reference for the other radiometers in the GPM constellation. There is no evidence of solar intrusions, an emissive reflector, calibration nonlinearities, warm load problems, or other issue impacting previous radiometers.
   - Corrections for calibration issues have been developed and applied for several of the radiometers. These include TMI emissive reflector and solar impacts on SSMIS. The initial intercalibration for all of the sensors relative to GMI are currently being finalized for delivery to the PPS.
   - A number of monitoring products are updated daily to identify potential issues with the raw count/Ta data, the calibration stability, and the ocean precipitation estimates (http://rain.atmos.colostate.edu/XCAL). This has helped identify the failure of the F16 SSMIS 183 GHz channels in December 2014 and the 150 GHz channel in May 2015.
2. Impacts on the Retrieval Algorithm
   - Differences in channel complements and spatial resolution have the largest impact on the resulting distribution of precipitation intensity. The GMI high-frequency channels in particular are very useful for improving snowfall detection and intensity.
   - AMSR2 retrievals over ocean are significant higher than for the other sensors. The AMSR2 nonlinearity correction appears to be at least part of the issue, but this has not yet been fully resolved.
3. Regime-dependent biases in the precipitation retrievals
   - See poster by Henderson et al. "Examining Regime Dependency of Z-R Relationships: Observations from Kwajalein, RMI"

CONTACT INFO

Wesley Berg
Dept. of Atmospheric Science
Fort Collins, CO 80523-1371
(970) 491-3443
berg@atmos.colostate.edu

Colorado State University